

FriendNet: Detection-Friendly Dehazing Network

Yihua Fan, Yongzhen Wang, Mingqiang Wei, *Senior Member, IEEE*, Fu Lee Wang, *Senior Member, IEEE*, and Haoran Xie, *Senior Member, IEEE*

Abstract—Adverse weather conditions often impair the quality of captured images, inevitably inducing cutting-edge object detection models for advanced driver assistance systems (ADAS) and autonomous driving. In this paper, we raise an intriguing question – can the combination of image restoration and object detection enhance detection performance in adverse weather conditions? To answer it, we propose an effective architecture that bridges image dehazing and object detection together via guidance information and task-driven learning to achieve detection-friendly dehazing, termed FriendNet. FriendNet aims to deliver both high-quality perception and high detection capacity. Different from existing efforts that intuitively treat image dehazing as pre-processing, FriendNet establishes a positive correlation between these two tasks. Clean features generated by the dehazing network potentially contribute to improvements in object detection performance. Conversely, object detection crucially guides the learning process of the image dehazing network under the task-driven learning scheme. We shed light on how downstream tasks can guide upstream dehazing processes, considering both network architecture and learning objectives. We design Guidance Fusion Block (GFB) and Guidance Attention Block (GAB) to facilitate the integration of detection information into the network. Furthermore, the incorporation of the detection task loss aids in refining the optimization process. Additionally, we introduce a new Physics-aware Feature Enhancement Block (PFEB), which integrates physics-based priors to enhance the feature extraction and representation capabilities. Extensive experiments on synthetic and real-world datasets demonstrate the superiority of our method over state-of-the-art methods on both image quality and detection precision. Our source code is available at <https://github.com/fanyihua0309/FriendNet>.

Index Terms—FriendNet, image dehazing, detection-friendly, object detection, detection guidance, task-driven

I. INTRODUCTION

IMAGES captured by outdoor vision systems, such as Unmanned aerial vehicles (UAVs), traffic monitoring, and surveillance, often face inevitable degradation [1]. Despite the effectiveness of leading vision approaches such as object detection [2] and vehicle re-identification [3], they struggle with the formidable challenges posed by hazy conditions [4]. This is primarily due to the degradation of visual quality, which severely hampers subsequent feature extraction and analysis

Y. Fan and M. Wei are with the School of Computer Science and Technology, Nanjing University of Aeronautics and Astronautics, Nanjing 210016, China, and also with the Shenzhen Institute of Research, Nanjing University of Aeronautics and Astronautics, Shenzhen 518038, China (e-mail: fanyihua@nuaa.edu.cn, mingqiang.wei@gmail.com).

Y. Wang is with the School of Computer Science and Technology, Anhui University of Technology, Ma'anshan 24303, China (e-mail: wangyz@ahut.edu.cn).

F. L. Wang is with the School of Science and Technology, Hong Kong Metropolitan University, Kowloon, Hong Kong SAR (e-mail: pwang@hkmu.edu.hk).

H. Xie is with the Department of Computing and Decision Sciences, Lingnan University, New Territories, Hong Kong SAR (e-mail: hrxie2@gmail.com).

in downstream tasks. Therefore, we attempt to explore how to obtain high-quality restoration results while simultaneously improving detection accuracy under degraded conditions.

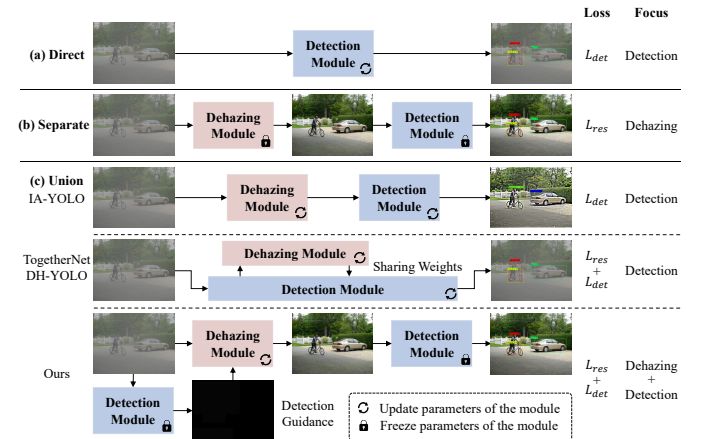


Fig. 1. Three primary categories of methods for object detection in hazy conditions. (a) Direct: detectors are trained directly on hazy images. (b) Separate: dehazing models serve as a pre-processing step, restoring images before feeding them into subsequent detectors. (c) Union: methods that concurrently address dehazing and detection under a unified pipeline (including IA-YOLO [5], TogetherNet [6], DH-YOLO [7] and the proposed FriendNet). These methods differ in terms of training losses and the decision to freeze or update the dehazing or detection module. Previous wisdom only focuses on optimizing one aspect of performance. Our FriendNet uniquely emphasizes the enhancement of both restoration quality and detection accuracy.

In previous studies, efforts to improve detection accuracy in hazy conditions typically fall into three categories, as illustrated in Fig. 1. One straightforward solution is to train and evaluate detectors directly on hazy images. However, the presence of blurring and occlusion in degraded images poses challenges for detectors to learn essential features, inevitably leading to poor performance. A prevalent strategy is to initially pre-process hazy images through existing dehazing algorithms [8]–[11]. Subsequently, the restored images are fed into the detection network for bounding box regression. Albeit images processed with dehazing algorithms exhibit better visual quality, they may not confer the same benefits upon high-level computer vision tasks. Recent research [7], [12]–[14] also reveals that there is no apparent correlation between the visual quality of dehazed images and the accuracy of object detection. We consider that the reason is rooted in the divergent objectives of restoration and detection, which can cause potential conflicts between them. Images generated by restoration models may contain imperceptible noise and unintentionally lose crucial details, potentially hindering the performance of subsequent detection models.

To tackle this challenge, a more effective solution lies in the pursuit of a unified paradigm that establishes connections

between low-level image dehazing and high-level object detection, indicating the relation and influence between them. Only a limited number of works [15]–[18] have ventured into this challenging direction. IA-YOLO [5] incorporates an image processing module into a YOLO detector to adaptively enhance each hazy image for better detection performance. DSNet [19], TogetherNet [6], and DH-YOLO [7] integrate an additional feature recovery branch to learn clean features. The feature extraction layers are shared between this branch and the detection backbone, thus facilitating the detection. Despite the promising results yielded by previous methods, attention has been narrowly focused on optimizing one aspect of performance. Some methods concentrate solely on the dehazing task, ignoring whether the dehazing results could improve detection performance. Conversely, other methods exclusively assess the detection performance and overlook the restoration quality, thereby compromising their practical applicability in scenarios where the quality of restored results is equally crucial. The precise mechanism for optimizing both low-level and high-level tasks remains unclear and intricate. Therefore, the design of a unified optimization paradigm emerges as a pivotal research direction.

Moving beyond previous wisdom, we uniquely place emphasis on enhancing both restoration quality and detection accuracy. Our approach offers a fresh perspective to investigate the potential advantage of leveraging detection prediction information and task-driven learning to better guide the dehazing process, thereby resulting in improvements in downstream detection accuracy. The interaction between low-level dehazing and high-level detection occurs bidirectionally. On one hand, clean features generated by the dehazing network potentially contribute to improvements in object detection performance. On the other hand, object detection crucially guides the learning process of the image dehazing network. The two tasks yield mutual benefits within a unified deep learning framework that connects image dehazing and object detection, termed FriendNet. FriendNet comprises two core components, i.e., the dehazing network and the detection network. Considering the impressive capabilities of YOLOv7 in object detection, we opt for YOLOv7-tiny, the most compact version of the YOLOv7 family, as the detector to facilitate deployments.

Specifically, we commence by pre-training the detector and maintaining its parameters fixed while updating the dehazing network. Given a hazy input image, we employ the frozen detector to obtain detection predictions, which may contain crucial information that could facilitate the dehazing optimization process. Hence, we derive detection guidance resembling a mask image from the predictions. In pursuit of detection-friendly objectives, we integrate the information conducive to detection into the dehazing learning process, considering both network structure and learning objectives.

Taking into account the network architecture, we design two key components, namely Guidance Fusion Block (GFB) and Guidance Attention Block (GAB) to fully leverage detection guidance. They offer instructive cues to the dehazing network at both coarse and fine levels. Moreover, we develop the Physics-aware Feature Enhancement Block (PFEB) which leverages the inherent understanding of the atmospheric scat-

tering model in the feature space. It enhances the capabilities of our model in feature extraction and representation. Absorbing both the physics-based prior and guidance wisdom, the feature maps generated by the dehazing network tend to estimate more essential features that are beneficial for both dehazing and detection. In terms of optimization objectives, we consider not only the regular restoration loss but also a detection loss. This additional loss term encourages the model to be more adept at facilitating detection within a task-driven learning paradigm. With detection guidance and task-driven learning, FriendNet ultimately achieves both high-quality perception and outstanding detection capacity.

Extensive experiments conducted on both synthetic datasets and real-world hazy images demonstrate the superiority of our FriendNet over existing state-of-the-art approaches. In summary, our primary contributions are three-fold:

- We propose an effective and unified deep learning framework designed for detection-friendly dehazing, named FriendNet. By leveraging detection guidance and the task-driven learning paradigm, FriendNet ensures the dehazing network is optimized for detection, leading to outstanding detection capacity.
- We propose a Physics-aware Feature Enhancement Block (PFEB) which integrates physics-based priors into our fundamental dehazing block. This module enhances the feature extraction and representation abilities of FriendNet, resulting in visually pleasing dehazing outcomes and offering benefits for detection tasks.
- Through extensive comparisons with various state-of-the-art approaches across direct, separate, and union categories, FriendNet consistently exhibits its superiority, emerging as a promising new solution in this field.

II. RELATED WORK

A. Image Dehazing

Image dehazing, aiming to recover clean scenes from corresponding hazy images, has attracted significant attention over the past decade. Image dehazing solutions are generally categorized into prior-based and learning-based methods. Traditional methods typically rely on hand-crafted priors, such as the dark channel prior (DCP) [20], color attenuation prior [21], non-local prior [22], etc. However, these empirical priors exhibit limited practical capacity in handling complex and diverse hazy scenes.

The rapid advancement of deep learning has propelled learning-based methods to the forefront in recent years. Some approaches [23] combine CNN with the atmospheric scattering model, which separately estimates global atmospheric light and transmission map. AOD-Net [24] stands out by predicting a single output that jointly represents the atmospheric light and transmission map through a lightweight network. GridDehazeNet [25] proposes a grid-like multi-scale network architecture, which directly learns the haze-free feature map rather than estimating the transmission map. This shift has triggered a new trend where methods aim to estimate haze-free images or the residual between hazy and haze-free images. Subsequently, many learning-based methods tend to design

intricate network architectures and attention mechanisms to improve the expressive capacity of networks. For instance, FFANet [8] incorporates feature attention blocks, leveraging both channel and pixel attention to boost haze removal. AECR-Net [9] reuses the feature attention mechanism and proposes a contrastive regularization, drawing benefits from both positive and negative samples. C²PNet [10] further applies a curricular contrastive regularization that considers the difficulty of different negatives and enforces physics-based priors in the feature space. gUNet [11] and SFNet [26] represent a series of methods that develop variations of U-Net [27] with certain modifications. Despite the notable progress these methods have made in dehazing tasks, their emphasis solely revolves around enhancing image quality, often neglecting their broader impact on downstream tasks. In this paper, we investigate a solution aimed at establishing a positive correlation between low-level dehazing and high-level detection.

B. Object Detection

As a pivotal task in the realm of computer vision, object detection has gained substantial research attention in both academic and industrial communities. Current methods for object detection can fall into two categories, namely region proposal-based and regression-based approaches [28]. Region proposal-based methods typically entail generating regions of interest (ROIs) from an input image and then conducting object localization and classification on these candidate regions. Among them, R-CNN [29] represents a pioneering approach. Subsequently, Fast R-CNN [30] and Faster R-CNN [31] further strengthen speed and accuracy. Albeit their impressive detection accuracy, region proposal-based approaches often fall short in terms of inference speed, making them less suitable for real-time applications.

In contrast to region proposal-based methods, regression-based methods treat object detection as a regression problem, directly predicting bounding box coordinates and classification probabilities with a single CNN. The single shot multibox detector (SSD) [32] addresses the challenge of detecting small objects by leveraging VGG16 [33] to extract hierarchical feature maps from different layers to detect objects at different scales. RetinaNet [34] achieves superior accuracy by introducing focal loss and a feature pyramid network for multiscale predictions. The YOLO series [35]–[40] stands out as representative detectors, which achieves real-time detection and superior accuracy by simultaneously handling classification and localization. In a nutshell, regression-based detectors are generally faster, but their detection performance may slightly lag behind region proposal-based detectors. In this paper, we employ the advanced YOLOv7-tiny (the smallest version of the YOLOv7 family) as the detector. This offers additional guidance for the dehazing network to optimize itself in a manner conducive to detection tasks.

C. Object Detection in Adverse Weather

In contrast to the extensive research efforts dedicated to general object detection, relatively few studies have ventured into the challenging realm of object detection under adverse

weather conditions. Some methods [41]–[44] directly train and evaluate detection models on degraded datasets. However, the presence of blurring and occlusion in degraded images hinders the ability of models to learn essential detection features. One prevailing strategy is to pre-process degraded images by existing dehazing algorithms to enhance the visual quality before feeding them into the subsequent object detection network. Despite the improved overall quality, it does not necessarily guarantee a significant boost in detection performance. Previous studies have revealed a weak correlation between image quality and detection accuracy [7], [12]–[14].

Moving forward, some methods [45] cast object detection in adverse weather as a domain adaption task, transitioning from a source domain (clean images) to a target domain (degraded images). Since images captured in adverse weather inherently suffer from an obvious domain shift problem. Adversarial training is primarily employed to align the target features with the source features. An alternative trend involves joint training and optimization on degraded images. IA-YOLO [5] proposes a novel Image-Adaptive YOLO (IA-YOLO) framework, where each image can be adaptively enhanced for better detection performance. DSNet [19] integrates a feature recovery module that aims at visibility enhancement for detection, sharing feature extraction layers with the detection subnet. Furthermore, TogetherNet [6] develops a multi-task joint learning paradigm that concurrently handles image restoration and object detection. Lee et al. [18] introduce a task-driven training strategy that guides the high-level task model suitable for both image restoration and accurate perception. However, achieving universality and robustness in such scenarios remains a formidable challenge. In this paper, inspired by the insights of [18], we present a task-driven learning paradigm infused with detection guidance to deliver high performance and fast convergence, enforcing the dehazing process to be more detection-friendly.

III. METHODOLOGY

To enhance both the image quality and the detection capabilities in adverse weather conditions, we present a solution that integrates image dehazing and object detection networks. Our method promotes a collaborative interaction between these two components, allowing them to mutually benefit from each other. This section provides an in-depth exploration of our proposed framework, named DFD-Net, highlighting its key modules in achieving detection-friendly dehazing and haze-resistant detection. We begin by presenting an overview of the framework architecture. Following this, we explore the specifics of the image dehazing network and the object detection network. We reveal how the detection guidance and task-driven learning contribute to the outcomes, indicating their respective roles and functionalities within the framework. Finally, we introduce the loss terms employed for optimizing our network geared towards high-quality restoration and highly accurate detection.

A. Overview of FriendNet

Previous research [7], [12]–[14] has revealed a notable limitation – directly sending recovered images generated by the

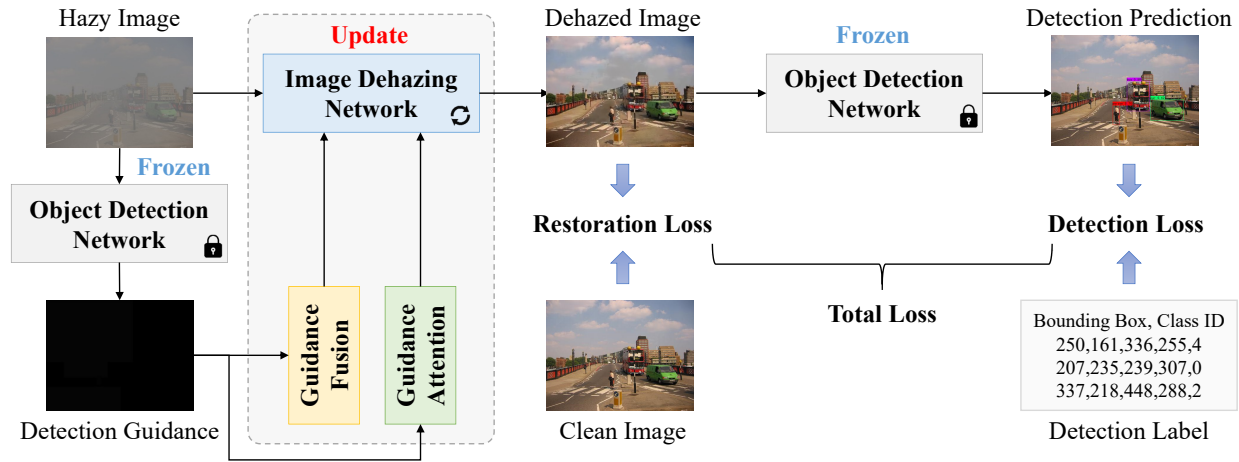


Fig. 2. Overview of our proposed framework. Our framework comprises an image dehazing network and an object detection network. These two components are integrated into a unified pipeline and trained in an end-to-end manner. The detector is pre-trained to offer additional wisdom for the optimization process of dehazing. It facilitates training through guidance fusion, guidance attention, and detection loss constraints.

dehazing network to the object detector does not necessarily lead to improved accuracy. In some cases, it may even result in a performance decline. This phenomenon is attributed to the observation that the restored image might compromise certain features inherent in the original hazy image and potentially create a new domain shift issue during the dehazing process. Consequently, this hinders the attainment of optimal performance when employing such a strategy.

In response to this challenge, we offer fresh insight to establish a positive relation between the image dehazing task and the object detection task to achieve mutual gain. With detection guidance feature fusion and attention mechanism, the feature maps produced by the dehazing network tend to pay more attention to the objects of interest. Besides, the introduction of detection loss serves to guide the dehazing network towards optimizing in a manner conducive to detection tasks. This strategy not only encourages attention to relevant objects but also promotes the dehazing network to align its optimization with the requirements of the subsequent detection task, thereby contributing to an overall improvement in performance.

The overall pipeline of the proposed FriendNet is depicted in Fig. 2. FriendNet consists of an image dehazing network and an object detection network. These two components collaborate within a unified pipeline and undergo end-to-end training for optimal performance. Given that the joint framework includes two sub-networks tailored for image dehazing and object detection tasks, it inevitably introduces more uncertainties to the training process if initializing them completely at random, which in turn makes the training converge slowly. To mitigate this issue, the detector is trained in advance and frozen during the learning process of dehazing, which ensures fast convergence and high performance of our method.

Specifically, given a hazy input image, the pre-trained detector is initially employed to obtain detection predictions. Acknowledging that these initial results may not be optimal, we discern the potential presence of valuable information that can guide the dehazing optimization process. Therefore, we generate a detection guidance which is a mask-like image

derived from the detection predictions. To effectively make use of this guidance, we design the Guidance Fusion Block (GFB) and the Guidance Attention Block (GAB). Additionally, we develop the Physics-aware Feature Enhancement Block (PFEB) which leverages the prior knowledge of the atmospheric scattering model in the feature space. Absorbing both the physics and guidance wisdom, the feature maps produced by the dehazing network tend to estimate more useful features which are beneficial both for dehazing and detection. Furthermore, we employ a high-level task loss from the pre-trained detector to provide the dehazing network with connectivity that promotes it to be detection-friendly.

B. Dehazing Network Architecture

Recently, deep learning-based methods [11], [26], [47] have demonstrated remarkable performance in image restoration tasks, with many of them being derived from the classical U-Net solution. Following the previous wisdom, we establish U-shaped architecture with skip connections. As illustrated in Fig. 3, the basic dehazing block within our framework is the Physics-aware Feature Enhancement Block (PFEB). This block operates as a two-stage feature extractor, encompassing both shallow and deep features. In each stage, the input feature undergoes normalization via a BatchNorm layer, leveraging its ability to accelerate network convergence, enhance generalization, and mitigate overfitting. The output is finally combined with the identity shortcut of the input feature.

In the first stage, drawing inspiration from gUNet-T [11], we employ a point-wise convolutional layer and a depth-wise convolutional layer to extract feature x . Subsequently, a point-wise convolutional layer coupled with a Sigmoid function operates as the gating signal for x . The output is then projected using an additional point-wise convolutional layer. The gating mechanisms are helpful in improving the expressive capability of networks, which has garnered widespread consensus in the realm of image restoration [47].

In the second stage, considering the prevailing influence of attention mechanisms in computer vision, existing methods [8]

itive performance. In our framework, we employ YOLOv7-tiny as the detector, which is the smallest version within the YOLOv7 family. Although larger detectors might offer increased detection capacity, we deliberately opt for a lightweight alternative to strike a favorable balance between computational efficiency and performance.

To ensure fast convergence and stable training, the object detection network YOLOv7-tiny is initially pre-trained. The network takes clean images as inputs and produces outputs containing object classes along with their corresponding location coordinates within the image. Subsequently, we maintain the parameters of the detector fixed during the training phase for image dehazing. Next, a crucial challenge arises: how do we effectively integrate the pre-trained detector and its initial predictions into the dehazing task? This will be demonstrated in the following section.

D. Detection Guidance Integration Modules

Our goal is to recover detection-friendly images with promising visual quality. The challenge lies in narrowing the objective gap between low- and high-level tasks. Drawing inspiration from [50], we comprehensively leverage the pre-trained detector to offer valuable guidance to FriendNet, considering both network structure and learning objectives. We primarily adopt three operations to fulfill detection guidance, illustrated schematically in Fig. 2. Guidance Fusion Block (GFB) and Guidance Attention Block (GAB) integrate the detection information into the network structure, while the detection loss L_{det} facilitates the optimization process.

Recognizing the limitations in the initial detection outcomes produced by YOLOv7-tiny, we discern the potential presence of valuable information that can serve as effective priors. They can indicate a more effective pattern, directing the focus of dehazing toward areas containing objects of interest. It aims to enrich the high-level scene understanding ability of the dehazing model throughout its training phase.

To implement this strategy, we generate a detection guidance image, denoted as g , serving as an auxiliary mask-like input to the dehazing network. It is initially set as an all-zero image, and then its values are determined by:

$$g(x, y) = \begin{cases} 0, & (x, y) \text{ not in } b \\ (\text{class ID} + 1) * \text{score}, & (x, y) \text{ in } b, \end{cases} \quad (3)$$

where (x, y) refers to the pixel coordinates, and b refers to the predicted bounding box. In areas within the bounding boxes, values are assigned with the product of the score and its class ID plus 1 (considering class ID starts from zero). This assignment enables differentiation between areas with and without objects, as well as among different objects, thereby providing valuable guidance for the dehazing network throughout the training process.

To give full play to the guidance of detection predictions, we elaborately design the Guidance Fusion Block (GFB) and the Guidance Attention Block (GAB). The schematic diagrams of GFB and GAB are depicted in Fig. 4. In particular, for GFB, we employ point-wise and depth-wise convolutional layers to extract latent features of g . To maintain consistency

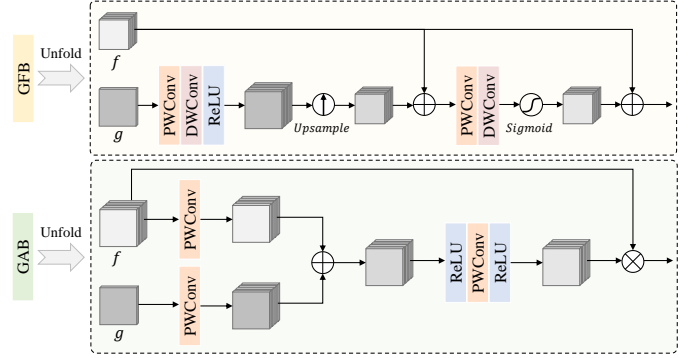


Fig. 4. The detailed structure of Guidance Fusion Block (GFB) and Guidance Attention Block (GAB). The integration of GFB and GAB into the dehazing network contributes to acquiring feature representations that are highly conducive to improved detection capabilities.

in resolution between the original feature and the guidance feature, an upsample operation is applied. The fused feature is obtained through their summation, enhancing the directional and effective propagation of shallow features. As for GAB, one point-wise convolutional layer is applied to the original feature f and guidance g , respectively. The combination proceeds through a ReLU function, a PWConv operation, and another ReLU function to derive the attention coefficient. Consequently, the output feature is obtained by multiplying f with the attention coefficient. This process transforms the feature maps of the detection guidance into attention, refining high-level features with greater specificity at the pixel level. GFB is employed for shallow feature maps, while GAB is utilized for deep feature maps, ensuring guidance from both coarse and fine levels, respectively.

In addition to offering instructive guidance to the network, we incorporate a high-level task loss to facilitate the optimization process of low-level image dehazing. The detection loss is imposed to endow the dehazing network with connectivity that encourages optimization toward a more detection-friendly direction. With the comprehensive exploration of cooperative strategies, three key operations, namely guidance fusion, guidance attention, and detection loss, harmonize to aggregate dehazing effects conducive to detection, considering both network structure and learning objectives.

E. Loss Function Design

Based on the above introduction, the total loss function for the network is defined as follows:

$$L_{total} = L_{res} + \lambda L_{det}, \quad (4)$$

where L_{res} denotes the loss function of the image restoration task, L_{det} denotes the loss function of the object detection task, and λ is a trade-off hyper-parameter to balance the significance of these two tasks. According to the ablation study on loss weights, we set λ at 0.4 to yield optimal performance.

To conduct image dehazing, the Mean Absolute Error (MAE) loss is employed to attain the estimated clean image. The Mean Square Error (MSE) loss tends to decrease gradient information for semantics, resulting in inferior performance,

as evidenced by our experiments. The restoration loss L_{res} can be expressed by:

$$L_{res} = \sum_{n=1}^N \|J - \hat{J}\|_1, \quad (5)$$

where N denotes the total number of training samples. J and \hat{J} denote the clean and estimated restored images, respectively.

To promote the dehazing optimization towards a more detection-friendly direction, we employ the detection loss of the original YOLOv7-tiny as L_{det} , which is expressed by:

$$L_{det} = \lambda_{box}L_{box} + \lambda_{obj}L_{obj} + \lambda_{cls}L_{cls}, \quad (6)$$

where L_{box} , L_{obj} , and L_{cls} refer to localization loss, confidence loss, and classification loss, respectively. The corresponding weight coefficients λ_{box} , λ_{obj} , and λ_{cls} adhere to the original configuration.

IV. EXPERIMENT

In this section, comprehensive experiments are performed to assess both the image quality and the detection performance of our proposed method in comparison to state-of-the-art methods in hazy scenes. To facilitate these experiments, we establish a synthetic dataset named VOC-FOG specifically designed for detecting objects in foggy weather. For evaluation, both synthetic and real-world datasets are employed as the testing set. Moreover, ablation studies are conducted to further validate the effectiveness of each module and loss function.

A. Dataset

1) *Training Set*: There are few publicly available datasets for object detection in adverse weather conditions. To overcome this, we establish a specialized benchmark for image dehazing geared toward object detection. Leveraging the well-known atmospheric scattering model, we simulate fog on the original VOC dataset [51] to create the VOC-Fog dataset.

The atmospheric scattering model is formulated as Eq. 1. The transmission map $t(x)$ in this model is calculated by:

$$t(x) = e^{-\beta \times d(x)}, \quad (7)$$

where β represents the hazy thickness level, and $d(x)$ refers to the scene depth, which can be calculated by:

$$d(x) = -0.04 \times \rho + \sqrt{\max(h, w)}, \quad (8)$$

where ρ refers to the Euclidean distance from the current pixel to the central pixel. h and w refer to the height and width of the image, respectively.

The synthesis process for a hazy image is outlined in Algorithm. 1. In our experiments, we set A to be 0.5, and β in the range between 0.07 and 0.12. Additionally, the starting point for synthesizing haze is chosen as the center of the image, as it typically corresponds to the position with the largest depth value. Consequently, the haze in the central area appears thicker than in the surrounding areas. Some examples from VOC-FOG are provided in Fig. 5.

Algorithm 1: Synthesis Process of a Hazy Image

Input: Clean image J , global atmospheric light A , hazy thickness level β .
Output: Synthesized hazy image I .
 // Get dimensions of the clean image
 1 $(h, w, _)$ = J.shape
 // Initialize the synthesized hazy image
 2 $I = J.copy()$
 // Compute the size and center of the image
 3 $size = \max(h, w)$
 4 $c_h = h // 2$
 5 $c_w = w // 2$
 // Apply atmospheric scattering to each pixel
 6 **for** i **in** $range(h)$ **do**
 7 **for** j **in** $range(w)$ **do**
 8 $d = -0.04 \times \sqrt{(i - c_h)^2 + (j - c_w)^2} + \sqrt{size}$
 9 $t = e^{-\beta \times d}$
 10 $I[i][j] = I[i][j] \times t + A \times (1 - t)$
 11 **end**
 12 **end**



Fig. 5. Some examples from the proposed VOC-FOG dataset. The first row presents the clean images, and the second row displays the corresponding synthetic hazy images.

2) *Testing Set*: For evaluation, the corresponding synthetic dataset, VOC-FOG-Test, is employed as the testing set. The synthesis process for VOC-FOG-Test follows the same procedure as VOC-FOG. The value of A remains set at 0.5, while β is chosen from the range of 0.05 to 0.14 to simulate the complexity and variability of real-world scenes.

Furthermore, to explore the generality of the proposed method in wild scenarios, a challenging real-world dataset, named the Foggy Driving dataset [52] is adopted. This dataset offers a comprehensive collection of real-world scenes annotated with five object categories: bicycle, bus, car, motorbike, and person. To ensure consistency between the training and testing phases, we specifically select images containing these categories from the VOC dataset. More statistical details about datasets are presented in Tab. I.

TABLE I
DETAILS OF TRAINING AND TESTING DATASETS.

Usage	Dataset	Type	Images	Bicycle	Bus	Car	Motorbike	Person	Instances
Train	VOC-FOG	Synthetic	9578	615	499	1673	632	14206	17625
Test	VOC-FOG-Test	Synthetic	2129	138	139	432	131	3258	4098
	Foggy Driving	Real	101	17	17	425	7	269	735

TABLE II
QUANTITATIVE COMPARISON RESULTS OF THE PROPOSED METHOD WITH STATE-OF-THE-ART METHODS ON THE SYNTHETIC VOC-FOG-TEST DATASET.
BOLD AND UNDERLINED INDICATE THE BEST AND THE SECOND BEST RESULTS, RESPECTIVELY.

Strategy	Method	Publication	PSNR	SSIM	Bicycle	Bus	Car	Motorbike	Person	mAP
Direct	YOLOv7-tiny* [40]	CVPR'23	/	/	69.01	85.90	79.73	72.84	83.08	78.11
Baseline	YOLOv7-tiny [40]	CVPR'23	/	/	67.94	85.00	78.09	69.08	81.31	76.28
Separate	DCP+YOLOv7-tiny [20]	TPAMI'10	13.79	0.735	69.18	86.94	76.69	72.05	82.85	78.14
	AOD-Net+YOLOv7-tiny [24]	ICCV'17	16.05	0.594	65.26	83.05	75.41	62.21	78.78	72.94
	MSBDN+YOLOv7-tiny [54]	CVPR'20	28.87	0.879	70.92	85.78	79.32	70.80	83.10	77.98
	FFA-Net+YOLOv7-tiny [8]	AAAI'20	25.37	0.895	70.09	86.40	79.36	73.81	83.19	78.57
	PSD+YOLOv7-tiny [55]	CVPR'21	30.99	0.944	70.44	86.87	80.07	73.76	83.50	78.93
	LD-Net+YOLOv7-tiny [56]	TIP'21	21.02	0.768	<u>67.18</u>	85.51	77.34	67.25	81.52	<u>75.76</u>
	gUNet-T+YOLOv7-tiny [11]	arXiv'22	<u>32.21</u>	<u>0.948</u>	68.32	86.89	80.00	73.75	<u>84.17</u>	78.63
SFNet+YOLOv7-tiny [26]	ICLR'23	26.80	0.911	68.73	87.33	<u>79.74</u>	72.69	83.24	78.35	
Union	IA-YOLO [5]	AAAI'22	/	/	31.13	53.84	40.63	35.16	67.82	45.72
	TogetherNet [6]	CGF'22	/	/	68.92	83.94	77.46	70.57	83.25	76.83
	DH-YOLO [7]	ICANN'23	/	/	58.75	83.32	78.29	66.42	84.53	74.26
	Ours	/	32.93	0.951	70.92	<u>87.25</u>	79.86	74.91	83.61	79.31

B. Implementation Details

1) *Training Details*: The experiments are implemented using Pytorch on an NVIDIA GeForce RTX 2080 Ti GPU. The model is trained by the AdamW optimizer with a batch size of 16. The initial learning rate is set to 4×10^{-4} , and the learning rate is adjusted using a cosine annealing decay strategy. The training images are randomly cropped into 256×256 patches. We set the total number of epochs to 100 with 16,384 samples processed per epoch. Mixed precision training is enabled to increase the mini-batch size and reduce the training time.

2) *Evaluation Metrics*: To quantitatively evaluate the performance of our proposed method, we employ Peak Signal-to-Noise Ratio (PSNR) and Structural Similarity (SSIM) [53] to assess the image quality. In terms of the object detection task, we adopt the mean Average Precision (mAP) as the evaluation criterion with a confidence threshold of 0.5. Higher values of PSNR, SSIM, and mAP indicate better performance.

C. Comparisons with State-of-the-Arts

We conduct a comprehensive comparative analysis of the proposed method against several state-of-the-art approaches, with YOLOv7-tiny [40] serving as the baseline detector. The existing methods fall into the following three categories:

- 1) **Direct**: Hazy images are directly employed to train the detection model, denoted as YOLOv7-tiny* to distinguish it from YOLOv7-tiny trained on clean images;
- 2) **Separate**: Several dehazing algorithms are adopted as a pre-processing step, followed by object detection using YOLOv7-tiny trained on clean images. We select 8 popular dehazing methods, namely DCP [20], AOD-Net

[24], MSBDN [54], FFA-Net [8], PSD [55], LD-Net [56], gUNet-T [11] and SFNet [26];

- 3) **Union**: This category comprises methods that jointly consider low-level and high-level tasks and are trained on hazy images. We select 3 advanced methods, namely IA-YOLO [5], TogetherNet [6], and DH-YOLO [7].

All the methods are re-trained on our VOC-FOG dataset with recommended settings for fair comparisons.

1) *Comparisons on Synthetic Dataset*: The qualitative comparisons are illustrated in Fig. 6, with the respective PSNR and SSIM values presented below each image. Some methods, such as DCP, AOD-Net, and LD-Net exhibit limitations in completely removing haze. MSBDN tends to sacrifice details, resulting in a blurred appearance. Other methods introduce artifacts and amplify noise throughout the image. Our proposed FriendNet stands out by delivering superior perceptual quality compared to existing state-of-the-art methods.

The quantitative comparison results of FriendNet and state-of-the-art approaches on the synthetic VOC-FOG-Test dataset are presented in Tab. II. Among separate-category methods, such as AOD-Net and LD-Net, despite the improvement in image quality after dehazing, there is a noticeable decline in detection performance. This observation reveals the absence of a strong cause-and-effect relationship between image quality improvement and detection accuracy. Remarkably, our FriendNet demonstrates superior performance in both image dehazing and object detection. It is worth mentioning that the detection performance of YOLOv7-tiny on clean images stands at 79.70, and our method achieves dehazing results with only a minimal gap (0.39) compared to clean images.

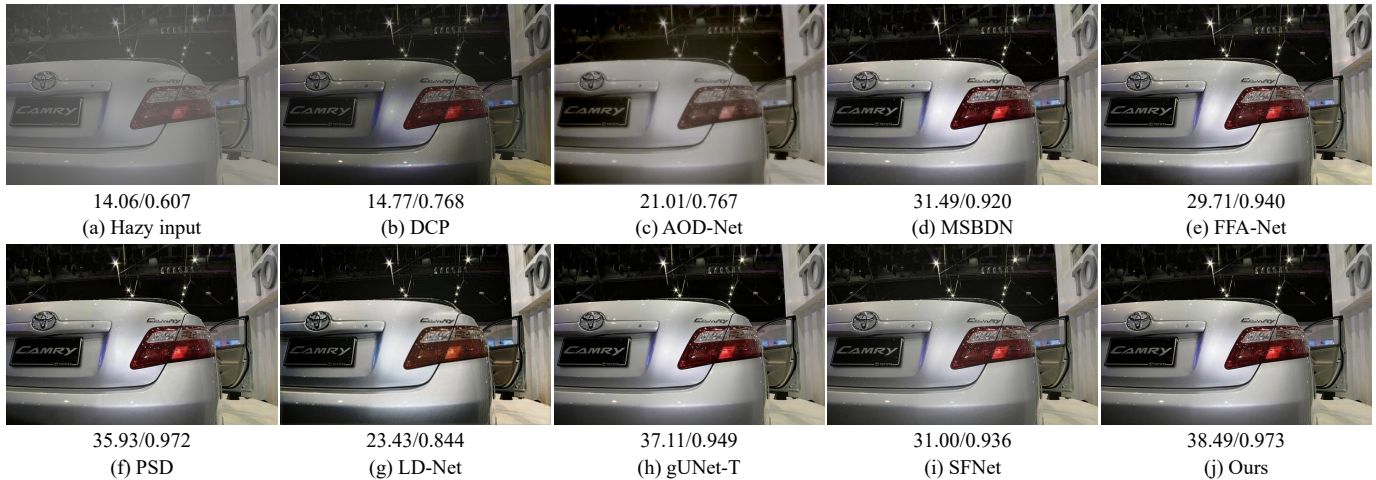


Fig. 6. Image dehazing results on VOC-FOG-Test. From (a) to (j): (a) the hazy image, and the dehazing outcomes of (b) DCP [20], (c) AOD-Net [24], (d) MSBDN [54], (e) FFA-Net [8], (f) PSD [55], (g) LD-Net [56], (h) gUNet-T [11], (i) SFNet [26], and (j) our FriendNet, respectively. PSNR and SSIM values are provided below each image. Our FriendNet can generate clearer and visually pleasing images.

TABLE III
 QUANTITATIVE COMPARISON RESULTS OF THE PROPOSED METHOD WITH STATE-OF-THE-ART METHODS ON THE REAL-WORLD FOGGY DRIVING DATASET. **BOLD** AND UNDERLINED INDICATE THE BEST AND THE SECOND BEST RESULTS, RESPECTIVELY.

Method	Bicycle	Bus	Car	Motorbike	Person	mAP
YOLOv7-tiny*	35.29	30.92	61.68	14.29	31.27	<u>34.69</u>
YOLOv7-tiny	<u>36.57</u>	34.12	<u>63.59</u>	4.76	30.10	33.83
DCP+YOLOv7-tiny	31.15	37.00	62.73	0.00	30.28	32.23
AOD-Net+YOLOv7-tiny	33.79	27.01	53.54	0.00	26.22	28.11
MSBDN+YOLOv7-tiny	32.13	37.97	58.75	7.14	30.53	33.30
FFA-Net+YOLOv7-tiny	<u>38.73</u>	33.92	61.25	0.00	29.77	32.73
PSD+YOLOv7-tiny	36.76	40.28	54.56	0.00	25.12	31.35
LD-Net+YOLOv7-tiny	37.08	<u>37.67</u>	53.46	<u>7.14</u>	30.80	33.23
gUNet-T+YOLOv7-tiny	38.57	32.41	60.80	0.00	30.56	32.47
SFNet+YOLOv7-tiny	36.27	33.72	63.74	3.57	30.53	33.57
IA-YOLO	11.67	5.28	30.63	0.00	11.46	10.75
TogetherNet	30.72	29.11	56.03	3.57	29.88	29.86
DH-YOLO	23.68	45.38	55.29	0.00	21.98	29.27
Ours	42.03	36.66	63.36	14.29	32.21	37.71

2) *Comparisons on Real-world Datasets:* To further investigate the applicability of the proposed method across diverse real-world scenarios, we conduct a comparative analysis between FriendNet and several cutting-edge methods on a challenging real-world dataset, namely Foggy Driving. As presented in Tab. III, our approach consistently maintains a leading position among state-of-the-art methods, achieving the highest mAP values and surpassing the second-best method by a significant margin (3.02 on mAP).

For qualitative detection comparisons, we select images from both synthetic and real-world datasets as test samples. The visualization of detection results is depicted in Fig. 7. Our method is compared with cutting-edge models, including YOLOv7-tiny, SF-Net+YOLOv7-tiny, IA-YOLO, TogetherNet, and DH-YOLO. Notably, FriendNet delivers more satisfactory visualization results compared to methods employing the separate strategy, along with a notable improvement in detecting more objects with higher confidence levels. This observation verifies the effectiveness of our proposed method in handling both synthetic and real-world hazy scenes, show-

ing its superior generalizability.

TABLE IV
 THE COMPUTATIONAL OVERHEAD COMPARISONS OF THE PROPOSED METHOD WITH STATE-OF-THE-ART IMAGE DEHAZING METHODS TESTED ON AN IMAGE WITH A RESOLUTION OF 256×256 PIXELS.

Method	Parameters (M)	FLOPs (G)	Latency (ms)
AOD-Net	0.002	0.11	0.20
MSBDN	31.35	41.52	14.03
FFA-Net	4.46	287.53	70.52
PSD	5.32	288.48	74.50
LD-Net	0.03	1.97	1.18
gUNet-T	0.84	2.81	4.74
SFNet	13.23	125.06	59.43
Ours	1.59	5.00	9.00

3) *Comparisons on Computational Efficiency:* Given the substantial disparity between the tasks of image dehazing and object detection, it is unjust to compare their computational overheads together. The proposed method essentially serves as a dehazing solution specifically designed for detection-friendly

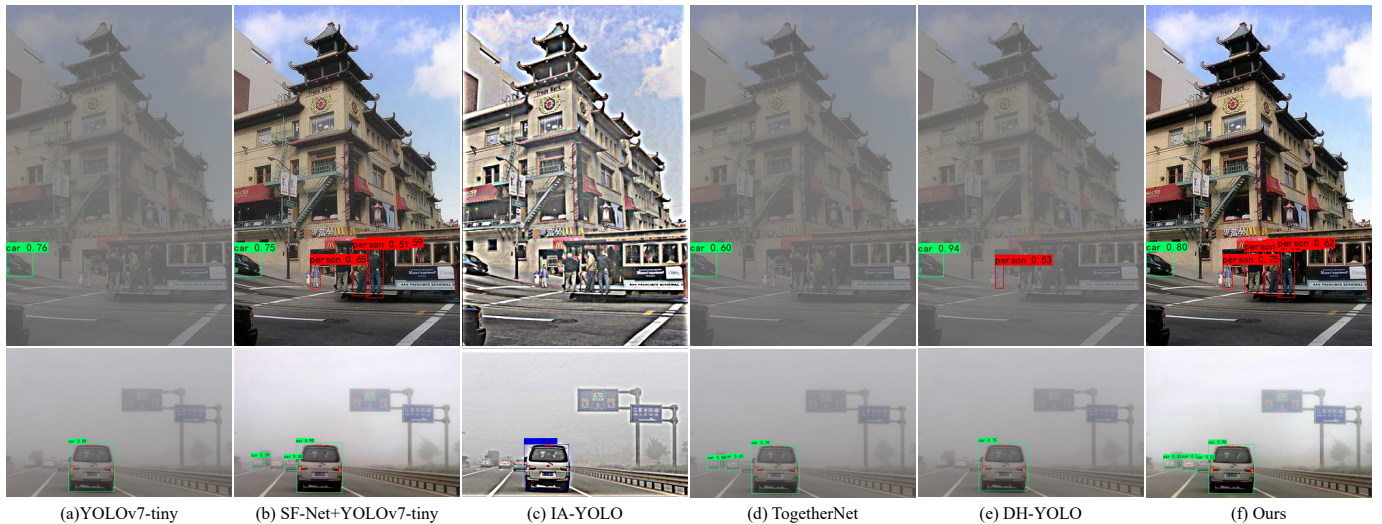


Fig. 7. Detection results by different methods on both synthetic and real-world foggy datasets. From (a) to (f): the detection results by (a) YOLOv7-tiny [40], (b) SF-Net+YOLOv7-tiny [26], (c) IA-YOLO [5], (d) TogetherNet [6], (e) DH-YOLO [7], and (f) our FriendNet, respectively. Clearly, FriendNet can discern more objects with higher confidence.

dehazing. Therefore, we exclusively measure the computational efficiency with state-of-the-art image dehazing methods for fair comparisons. The number of parameters, the number of floating-point operations (FLOPs), and latency serve as the primary indicators of computational efficiency. The results are reported in Tab. IV. Note that FLOPs are computed on a color image with a resolution of 256×256 pixels. The earlier dehazing method (i.e., AOD-Net) and the lightweight design (i.e., LD-Net) contain considerably small parameter sizes at the cost of a notable performance decline. Compared with recent SOTA methods, our FriendNet introduces an acceptable overhead compared to gUNet-T (0.75 increase in parameters and 2.19 increase in FLOPs). However, this modest increase in computational load leads to a substantial improvement in performance, as evidenced by a 5.24 gain in mAP on Foggy Driving. This implies the ability of FriendNet to strike a favorable balance between performance and model complexity.

D. Ablation Study

1) *Ablation on Network Components:* To further investigate the effectiveness of the proposed method, we conduct extensive ablation studies to analyze different components. We systematically eliminate each of the key components of the proposed FriendNet and establish several variants, including:

- 1) w/o PFEB_{s₂}: remove the second stage of feature extraction process in Physics-aware Feature Enhancement Block (PFEB);
- 2) w/o GFB: remove Guidance Fusion Block (GFB);
- 3) w/o GAB: remove Guidance Attention Block (GAB);
- 4) MAE \rightarrow MSE: replace the restoration loss from Mean Absolute Error (MAE) to Mean Squared Error (MSE);
- 5) w/o L_{det} : remove the object detection loss L_{det} .

All these variants are retrained in the same way as previously described. The quantitative results of ablation studies on network components are presented in Tab. V. Evidently, the full model stands out as the best-ranked approach that

outperforms the other variants. Each component introduced in our method significantly contributes to performance enhancement. Notably, the absence of the second stage in the feature extraction process in PFEB results in the model exhibiting poor performance on VOC-FOG-Test, with a 3.31 mAP drop in Foggy Driving. This emphasizes the effectiveness of incorporating physics priors into the feature space. Furthermore, the model trained without GFB and GAB experiences significant performance drops of 1.93 and 3.11 mAP on Foggy Driving, respectively. This reveals the crucial role of integrating detection guidance. In terms of loss functions, the model trained with MSE loss exhibits the least favorable performance, indicating the suitability for our network and its capacity to deliver superior results. Moreover, the model trained without the detection loss leads to a 3.33 mAP drop on Foggy Driving, highlighting the effectiveness of the task-driven learning paradigm. These findings collectively demonstrate the rationality and validity of our framework, which incorporates the feature enhancement module while leveraging detection guidance and high-level detection loss.

TABLE V
QUANTITATIVE RESULTS OF ABLATION STUDIES ON NETWORK COMPONENTS. **BOLD** INDICATES THE BEST RESULTS.

Variant	VOC-FOG-Test			Foggy Driving mAP
	PSNR	SSIM	mAP	
w/o PFEB _{s₂}	32.79	0.950	78.90	34.40
w/o GFB	31.98	0.944	79.08	35.78
w/o GAB	32.64	0.948	79.04	34.60
MAE \rightarrow MSE	29.57	0.920	78.67	35.24
w/o L_{det}	32.62	0.949	79.18	34.38
Ours	32.93	0.951	79.31	37.71

2) *Ablation on Loss Weights:* The loss function for the entire framework is a combination of both image restoration and object detection. Given the significant differences in magnitude and learning difficulty among various tasks, we

aim to find the optimal balance between restoration loss and detection loss. As formulated in Eq. 4, the weight of the restoration loss is fixed at 1.0. Comparison results for different values of the balancing parameter λ are presented in Tab. VI. As observed, we explore λ within the range of 0.01 to 10. Since the primary objective is to update the dehazing network, setting λ to large values, such as 10, inevitably introduces challenges in convergence, thereby leading to extremely poor outcomes. A more suitable value for λ is below 1.0, indicating a smaller weight than that of the restoration loss. Based on the analysis of experimental results, we set λ to 0.4 to yield the optimal detection performance. Although PSNR and SSIM do not reach their peak values under this configuration, the deviation from the optimum is minimal when compared to the best performance attained with λ set at 0.01.

TABLE VI
QUANTITATIVE RESULTS OF ABLATION STUDIES ON LOSS WEIGHTS.
BOLD INDICATES THE BEST RESULTS.

λ	VOC-FOG-Test			Foggy Driving
	PSNR	SSIM	mAP	mAP
0.01	32.9526	0.9513	79.23	35.67
0.1	32.5956	0.9507	79.28	35.51
0.2	32.9510	0.9506	78.83	36.46
0.4	32.9331	0.9506	79.31	37.71
0.5	32.8411	0.9492	79.16	35.93
0.6	32.8756	0.9506	78.98	34.78
1	32.3910	0.9475	79.21	35.52
10	21.7408	0.6070	51.84	27.76

E. Limitation and Discussion



Fig. 8. Failure cases. Our FriendNet faces challenges in handling images captured in extremely hazy conditions, where even humans have difficulty discerning all objects in such challenging scenarios.

Although our proposed method yields superior performance in both synthetic and real-world scenarios, it is essential to acknowledge certain failure cases. As illustrated in Fig. 8, our method faces challenges in handling extremely hazy degradations and struggles to successfully detect all objects in the image. It is noteworthy that even humans have difficulty discerning all the objects in such challenging scenarios. The

limited information available for the network makes it challenging to generate the missing details crucial for accurate detection in the neighborhood.

Moving forward, we are committed to addressing this limitation by exploring some powerful prior knowledge and integrating it into feature extraction modules. Furthermore, we intend to extend our current work to encompass other low-level and high-level tasks, aiming to investigate the versatility of our method. Through these efforts, we aspire to continually enhance the capability and applicability of our proposed method across various intricate and diverse settings.

V. CONCLUSION

In this paper, we propose an effective framework that assembles image dehazing and object detection to achieve detection-friendly dehazing, named FriendNet. From a fresh perspective, FriendNet investigates the potential advantages of building a positive interaction between low-level dehazing and high-level detection. It incorporates detection guidance into the dehazing network to generate features that are beneficial for detection. Furthermore, it employs a task-driven learning paradigm to endow the dehazing network with connectivity, encouraging optimization toward a more detection-friendly direction. In one direction, clean features produced by the dehazing network have the potential to enhance object detection performance. In the opposite direction, the object detection network can provide valuable information and conversely guide the learning process of dehazing. It reveals that low-level and high-level tasks can jointly promote each other and realize mutual gains. Additionally, we leverage physics-based priors to boost the feature extraction and representation capabilities of our model. Comprehensive experiments demonstrate the superiority of FriendNet in obtaining visually pleasing and realistic output images. The application of object detection further highlights our potential in settling and improving the performance of the downstream task. FriendNet emerges as a promising solution for bridging low-level and high-level tasks.

REFERENCES

- [1] Y. Wang, X. Yan, D. Guan, M. Wei, Y. Chen, X.-P. Zhang, and J. Li, "Cycle-snsrgan: Towards real-world image dehazing via cycle spectral normalized soft likelihood estimation patch gan," *IEEE Transactions on Intelligent Transportation Systems*, vol. 23, no. 11, pp. 20368–20382, 2022.
- [2] Q. Ding, P. Li, X. Yan, D. Shi, L. Liang, W. Wang, H. Xie, J. Li, and M. Wei, "Cf-yolo: Cross fusion yolo for object detection in adverse weather with a high-quality real snow dataset," *IEEE Transactions on Intelligent Transportation Systems*, 2023.
- [3] W.-T. Chen, I.-H. Chen, C.-Y. Yeh, H.-H. Yang, J.-J. Ding, and S.-Y. Kuo, "Sjdl-vehicle: Semi-supervised joint defogging learning for foggy vehicle re-identification," in *Proceedings of the AAAI Conference on Artificial Intelligence*, vol. 36, no. 1, 2022, pp. 347–355.
- [4] N. Lyu, J. Zhao, P. Liu, L. Li, Y. He, T. Su, and J. Wen, "Scene-adaptive real-time fast dehazing and detection in driving environment," *IEEE Transactions on Intelligent Transportation Systems*, 2023.
- [5] W. Liu, G. Ren, R. Yu, S. Guo, J. Zhu, and L. Zhang, "Image-adaptive yolo for object detection in adverse weather conditions," in *Proceedings of the AAAI Conference on Artificial Intelligence*, vol. 36, no. 2, 2022, pp. 1792–1800.
- [6] Y. Wang, X. Yan, K. Zhang, L. Gong, H. Xie, F. L. Wang, and M. Wei, "Togethernet: Bridging image restoration and object detection together via dynamic enhancement learning," in *Computer Graphics Forum*, vol. 41, no. 7. Wiley Online Library, 2022, pp. 465–476.

- [7] K. Zhang, X. Yan, Y. Wang, and J. Qi, "Adaptive dehazing yolo for object detection," in *International Conference on Artificial Neural Networks*. Springer, 2023, pp. 14–27.
- [8] X. Qin, Z. Wang, Y. Bai, X. Xie, and H. Jia, "Ffa-net: Feature fusion attention network for single image dehazing," in *Proceedings of the AAAI conference on artificial intelligence*, vol. 34, no. 07, 2020, pp. 11 908–11 915.
- [9] H. Wu, Y. Qu, S. Lin, J. Zhou, R. Qiao, Z. Zhang, Y. Xie, and L. Ma, "Contrastive learning for compact single image dehazing," in *Proceedings of the IEEE/CVF Conference on Computer Vision and Pattern Recognition*, 2021, pp. 10 551–10 560.
- [10] Y. Zheng, J. Zhan, S. He, J. Dong, and Y. Du, "Curricular contrastive regularization for physics-aware single image dehazing," in *Proceedings of the IEEE/CVF Conference on Computer Vision and Pattern Recognition*, 2023, pp. 5785–5794.
- [11] Y. Song, Y. Zhou, H. Qian, and X. Du, "Rethinking performance gains in image dehazing networks," *arXiv preprint arXiv:2209.11448*, 2022.
- [12] B. Li, W. Ren, D. Fu, D. Tao, D. Feng, W. Zeng, and Z. Wang, "Benchmarking single-image dehazing and beyond," *IEEE Transactions on Image Processing*, vol. 28, no. 1, pp. 492–505, 2018.
- [13] Y. Li, Y. Liu, Q. Yan, and K. Zhang, "Deep dehazing network with latent ensembling architecture and adversarial learning," *IEEE Transactions on Image Processing*, vol. 30, pp. 1354–1368, 2020.
- [14] C. Li, H. Zhou, Y. Liu, C. Yang, Y. Xie, Z. Li, and L. Zhu, "Detection-friendly dehazing: Object detection in real-world hazy scenes," *IEEE Transactions on Pattern Analysis and Machine Intelligence*, 2023.
- [15] D. Liu, B. Wen, J. Jiao, X. Liu, Z. Wang, and T. S. Huang, "Connecting image denoising and high-level vision tasks via deep learning," *IEEE Transactions on Image Processing*, vol. 29, pp. 3695–3706, 2020.
- [16] M. Haris, G. Shakhnarovich, and N. Ukita, "Task-driven super resolution: Object detection in low-resolution images," in *Neural Information Processing: 28th International Conference, ICONIP 2021, Samur, Bali, Indonesia, December 8–12, 2021, Proceedings, Part V 28*. Springer, 2021, pp. 387–395.
- [17] K. Wang, T. Wang, J. Qu, H. Jiang, Q. Li, and L. Chang, "An end-to-end cascaded image deraining and object detection neural network," *IEEE Robotics and Automation Letters*, vol. 7, no. 4, pp. 9541–9548, 2022.
- [18] Y. Lee, J. Jeon, Y. Ko, B. Jeon, and M. Jeon, "Task-driven deep image enhancement network for autonomous driving in bad weather," in *2021 IEEE International Conference on Robotics and Automation (ICRA)*. IEEE, 2021, pp. 13 746–13 753.
- [19] S.-C. Huang, T.-H. Le, and D.-W. Jaw, "Dsnnet: Joint semantic learning for object detection in inclement weather conditions," *IEEE transactions on pattern analysis and machine intelligence*, vol. 43, no. 8, pp. 2623–2633, 2020.
- [20] K. He, J. Sun, and X. Tang, "Single image haze removal using dark channel prior," *IEEE transactions on pattern analysis and machine intelligence*, vol. 33, no. 12, pp. 2341–2353, 2010.
- [21] Q. Zhu, J. Mai, and L. Shao, "Single image dehazing using color attenuation prior," in *BMVC*, 2014.
- [22] D. Berman, S. Avidan *et al.*, "Non-local image dehazing," in *Proceedings of the IEEE conference on computer vision and pattern recognition*, 2016, pp. 1674–1682.
- [23] B. Cai, X. Xu, K. Jia, C. Qing, and D. Tao, "Dehazenet: An end-to-end system for single image haze removal," *IEEE transactions on image processing*, vol. 25, no. 11, pp. 5187–5198, 2016.
- [24] B. Li, X. Peng, Z. Wang, J. Xu, and D. Feng, "Aod-net: All-in-one dehazing network," in *Proceedings of the IEEE international conference on computer vision*, 2017, pp. 4770–4778.
- [25] X. Liu, Y. Ma, Z. Shi, and J. Chen, "Griddehazenet: Attention-based multi-scale network for image dehazing," in *Proceedings of the IEEE/CVF international conference on computer vision*, 2019, pp. 7314–7323.
- [26] Y. Cui, Y. Tao, Z. Bing, W. Ren, X. Gao, X. Cao, K. Huang, and A. Knoll, "Selective frequency network for image restoration," in *The Eleventh International Conference on Learning Representations*, 2023.
- [27] O. Ronneberger, P. Fischer, and T. Brox, "U-net: Convolutional networks for biomedical image segmentation," in *Medical Image Computing and Computer-Assisted Intervention—MICCAI 2015: 18th International Conference, Munich, Germany, October 5–9, 2015, Proceedings, Part III 18*. Springer, 2015, pp. 234–241.
- [28] Z.-Q. Zhao, P. Zheng, S.-t. Xu, and X. Wu, "Object detection with deep learning: A review," *IEEE transactions on neural networks and learning systems*, vol. 30, no. 11, pp. 3212–3232, 2019.
- [29] R. Girshick, J. Donahue, T. Darrell, and J. Malik, "Rich feature hierarchies for accurate object detection and semantic segmentation," in *Proceedings of the IEEE conference on computer vision and pattern recognition*, 2014, pp. 580–587.
- [30] R. Girshick, "Fast r-cnn," in *Proceedings of the IEEE international conference on computer vision*, 2015, pp. 1440–1448.
- [31] S. Ren, K. He, R. Girshick, and J. Sun, "Faster r-cnn: Towards real-time object detection with region proposal networks," *Advances in neural information processing systems*, vol. 28, 2015.
- [32] W. Liu, D. Anguelov, D. Erhan, C. Szegedy, S. Reed, C.-Y. Fu, and A. C. Berg, "Ssd: Single shot multibox detector," in *Computer Vision—ECCV 2016: 14th European Conference, Amsterdam, The Netherlands, October 11–14, 2016, Proceedings, Part I 14*. Springer, 2016, pp. 21–37.
- [33] K. Simonyan and A. Zisserman, "Very deep convolutional networks for large-scale image recognition," *arXiv preprint arXiv:1409.1556*, 2014.
- [34] T.-Y. Lin, P. Goyal, R. Girshick, K. He, and P. Dollár, "Focal loss for dense object detection," in *Proceedings of the IEEE international conference on computer vision*, 2017, pp. 2980–2988.
- [35] J. Redmon, S. Divvala, R. Girshick, and A. Farhadi, "You only look once: Unified, real-time object detection," in *Proceedings of the IEEE conference on computer vision and pattern recognition*, 2016, pp. 779–788.
- [36] J. Redmon and A. Farhadi, "Yolo9000: better, faster, stronger," in *Proceedings of the IEEE conference on computer vision and pattern recognition*, 2017, pp. 7263–7271.
- [37] A. Bochkovskiy, C.-Y. Wang, and H.-Y. M. Liao, "Yolov4: Optimal speed and accuracy of object detection," *arXiv preprint arXiv:2004.10934*, 2020.
- [38] G. Jocher, A. Chaurasia, A. Stoken, J. Borovec, Y. Kwon, K. Michael, J. Fang, Z. Yifu, C. Wong, D. Montes *et al.*, "ultralytics/yolov5: v7.0-yolov5 sota realtime instance segmentation," *Zenodo*, 2022.
- [39] C. Li, L. Li, H. Jiang, K. Weng, Y. Geng, L. Li, Z. Ke, Q. Li, M. Cheng, W. Nie *et al.*, "Yolov6: A single-stage object detection framework for industrial applications," *arXiv preprint arXiv:2209.02976*, 2022.
- [40] C.-Y. Wang, A. Bochkovskiy, and H.-Y. M. Liao, "Yolov7: Trainable bag-of-freebies sets new state-of-the-art for real-time object detectors," in *Proceedings of the IEEE/CVF Conference on Computer Vision and Pattern Recognition*, 2023, pp. 7464–7475.
- [41] J. Yim and K.-A. Sohn, "Enhancing the performance of convolutional neural networks on quality degraded datasets," in *2017 International Conference on Digital Image Computing: Techniques and Applications (DICTA)*. IEEE, 2017, pp. 1–8.
- [42] D. Hendrycks and T. Dietterich, "Benchmarking neural network robustness to common corruptions and perturbations," *arXiv preprint arXiv:1903.12261*, 2019.
- [43] M. Singh, S. Nagpal, R. Singh, and M. Vatsa, "Dual directed capsule network for very low resolution image recognition," in *Proceedings of the IEEE/CVF International Conference on Computer Vision*, 2019, pp. 340–349.
- [44] C. Wang, C. Li, B. Luo, W. Wang, and J. Liu, "Riwnet: A moving object instance segmentation network being robust in adverse weather conditions," *arXiv preprint arXiv:2109.01820*, 2021.
- [45] S. Zhang, H. Tuo, J. Hu, and Z. Jing, "Domain adaptive yolo for one-stage cross-domain detection," in *Asian Conference on Machine Learning*. PMLR, 2021, pp. 785–797.
- [46] J. Hu, L. Shen, and G. Sun, "Squeeze-and-excitation networks," in *Proceedings of the IEEE conference on computer vision and pattern recognition*, 2018, pp. 7132–7141.
- [47] L. Chen, X. Chu, X. Zhang, and J. Sun, "Simple baselines for image restoration," in *European Conference on Computer Vision*. Springer, 2022, pp. 17–33.
- [48] J. Dong and J. Pan, "Physics-based feature dehazing networks," in *Computer Vision—ECCV 2020: 16th European Conference, Glasgow, UK, August 23–28, 2020, Proceedings, Part XXX 16*. Springer, 2020, pp. 188–204.
- [49] D. Hendrycks and K. Gimpel, "Gaussian error linear units (gelus)," *arXiv preprint arXiv:1606.08415*, 2016.
- [50] T. Hong, X. Guo, Z. Zhang, and J. Ma, "Sg-net: Semantic guided network for image dehazing," in *Asian Conference on Computer Vision*. Springer, 2022, pp. 274–289.
- [51] M. Everingham, L. Van Gool, C. K. Williams, J. Winn, and A. Zisserman, "The pascal visual object classes (voc) challenge," *International journal of computer vision*, vol. 88, pp. 303–338, 2010.
- [52] C. Sakaridis, D. Dai, and L. Van Gool, "Semantic foggy scene understanding with synthetic data," *International Journal of Computer Vision*, vol. 126, pp. 973–992, 2018.

- [53] Z. Wang, A. C. Bovik, H. R. Sheikh, and E. P. Simoncelli, "Image quality assessment: from error visibility to structural similarity," *IEEE transactions on image processing*, vol. 13, no. 4, pp. 600–612, 2004.
- [54] H. Dong, J. Pan, L. Xiang, Z. Hu, X. Zhang, F. Wang, and M.-H. Yang, "Multi-scale boosted dehazing network with dense feature fusion," in *Proceedings of the IEEE/CVF conference on computer vision and pattern recognition*, 2020, pp. 2157–2167.
- [55] Z. Chen, Y. Wang, Y. Yang, and D. Liu, "Psd: Principled synthetic-to-real dehazing guided by physical priors," in *Proceedings of the IEEE/CVF conference on computer vision and pattern recognition*, 2021, pp. 7180–7189.
- [56] H. Ullah, K. Muhammad, M. Irfan, S. Anwar, M. Sajjad, A. S. Imran, and V. H. C. de Albuquerque, "Light-dehazenet: a novel lightweight cnn architecture for single image dehazing," *IEEE transactions on image processing*, vol. 30, pp. 8968–8982, 2021.



Yihua Fan is currently a Ph.D candidate with the School of Computer Science and Technology, Nanjing University of Aeronautics and Astronautics (NUAA). She received her B.S. degree from NUAA in 2022. Her research interests include deep learning, image processing, and computer vision.



Yongzhen Wang received the Ph.D. degree in Computer Science and Technology from the Nanjing University of Aeronautics and Astronautics (NUAA) in 2023. He is currently a Lecturer at the Anhui University of Technology, China. He has published more than 20 research papers, including IEEE TIP, IEEE TITS, IEEE TGRS, etc. His research interests include deep learning, computer vision, and image processing, particularly in the domains of object detection and image restoration. He has served as a PC Member for AAAI from 2022 to 2024.



Mingqiang Wei (Senior Member, IEEE) received his Ph.D degree (2014) in Computer Science and Engineering from the Chinese University of Hong Kong (CUHK). He is a professor at the School of Computer Science and Technology, Nanjing University of Aeronautics and Astronautics (NUAA). He is now an Associate Editor for ACM TOMM, The Visual Computer, and a Guest Editor for IEEE Transactions on Multimedia. His research interests focus on 3D vision, and computer graphics.



Fu Lee Wang (SM'15) received the B.Eng. degree in computer engineering and the M.Phil. degree in computer science and information systems from the University of Hong Kong, Hong Kong, and the Ph.D. degree in systems engineering and engineering management from the Chinese University of Hong Kong, Hong Kong. Prof. Wang is the Dean of the School of Science and Technology, at Hong Kong Metropolitan University, Hong Kong. He has over 290 publications in international journals and conferences and led more than 20 competitive grants with a total greater than HK\$20 million. His current research interests include educational technology, information retrieval, computer graphics, and bioinformatics. Prof. Wang is a fellow of BCS and HKIE and a Senior Member of ACM. He was the Chair of the IEEE Hong Kong Section Computer Chapter and ACM Hong Kong Chapter.



Haoran Xie (Senior Member, IEEE) received a Ph.D. degree in Computer Science from City University of Hong Kong and an Ed.D degree in Digital Learning from the University of Bristol. He is currently the Department Head and Associate Professor at the Department of Computing and Decision Sciences, Lingnan University, Hong Kong. His research interests include artificial intelligence, big data, and educational technology. He has published 400 research publications, including 226 journal articles such as IEEE TPAMI, IEEE TKDE, IEEE TAFCC, and IEEE TCVST. He is the Editor-in-Chief of Natural Language Processing Journal, Computers & Education: Artificial Intelligence and Computers & Education: X Reality. He has been listed as one of the World's Top 2% Scientists by Stanford University.